

Quasi-crystals as catalyst for steam reforming of methanol

Nagia Ahmad Ali Arfa
Assistant staff,
College of Engineering Technology / Janzur

e.mail:Najiaahmad691@gmail.com

Abstract

X-ray photoelectron spectroscopy (XPS) has been used with a view to analyzing the chemical composition and the state of oxidation of elements on the surface of Al-Cu-Fe and Al- Pd- Mn quasi-crystals. Al on both quasi-crystals surface has been decreased after sputtering with Argon. Therefore, due to Al oxide which formed on the surface which give rise to a shift in the binding energy of Al $2p$. As for other metals in both quasi-crystal samples, which represent in Fe, Cu, Pd and oxides have been observed on the surface. Metals oxidation plays an important role with respect to increasing the catalytic performance on the quasi-crystal surface. Further to this, following methanol deposition, the measurements of peak position of XPS spectra shown the presence of core level binding energy of C_{1s} shifts, due to methanol decomposition that has been taken place during this experiment.

Introduction

Quasi-crystal was discovered in 1984 by Shechtman [1, 2], via the investigation of rapidly solidified of Al- Mn alloys. The diffraction pattern obtained from the Al-Mn alloy showed sharp diffraction with five-fold symmetry peaks [3]. This pattern was attributed to the presence of long-range order with lack of periodicity and forbidden rotational symmetry, for instance 5-fold, 10-fold [4]. Currently, they have become attractive to use as catalysts, particularly in steam reforming of methanol applications (SRM). Tsai et al. reported that the Al-Cu-Fe QC powder showed a highly stable and active catalyst than its individual metal catalysts in the steam reforming of methanol, which can offer great opportunities to the hydrogen production industry [5]

Quasi-crystals are characterized by hard and brittle nature at room temperature [6] which result from the quasiperiodic structure, the thermodynamic equilibrium stability and their content of low cost materials for example Cu, Fe and Pd, which can be compared to the presence industrial catalyst as Pt [7]. These materials also provide advantageous properties over commercial catalysts, for example Pd has the resistance to oxidation at elevated temperature [8]. Finally, the range of hardness of quasi-crystal is harder than the individual components [4, 9].

Previous research undertaken has used a powder sample and the difficulties related to identification of their structure with the complexities, due to that. Therefore, this work will study the surface model of a single grain QCs to identify their structure to get insight into the surface behavior of catalyst reaction. The data from experiments will be analyzed by casa XPS including elemental peak position identification and quantification of the surface composition (required to be analyzed by a sensitive technique); X-ray photoelectron spectroscopy (XPS) and Ultra High Vacuum (UHV) will be used for operating the sputtering and annealing for cleaning samples. The experiments were attempted to investigate the surface structure of both

Al-Cu-Fe and Al-Pd-Mn QCs in terms of study how the active catalyst produce at the surface to the SRM reaction. Followed by investigate whether these quasi-crystals can be prepared to use as a model of catalyst. This report is organized as follows; section [sec: Steam reforming of methanol] will describe the steam reforming of methanol and our experimental methods will be discussed in section [sec: Experiment]. The results and discussion of the surface per sample are presented in section [sec: Result-and-discussion]. The conclusion will be presented in final section.

Steam Reforming of Methanol (SRM)

Methanol decomposed to carbon dioxide and hydrogen at a specific temperature around (500 K) [10] and with the presence of a suitable catalysts and these catalysts offer more opportunities to speed up this reaction and lead to produce the highest hydrogen (H₂) to carbon ratio.



The usage of Al-Cu-Fe powder which showed a highly stable and active catalyst than its individual metal catalysts in SRM and the rate of producing H₂ after leaching treatment was 235 l/Kg per minute which represents high production rate whether compared with that was produced commercially [5].

Experiment methods and techniques

X-ray photoelectron spectroscopy (XPS)

X-ray photoelectron spectroscopy (XPS) is the most widespread surface science technique for analyzing the photoemission that based upon Einstein's photoelectric effect which was proposed in 1905. An XPS spectrum is a technique which records electrons that have been emitted from atoms excited by incident photons (X-ray radiation) Figure (1). Electrons with a wide range of kinetic energies (K.E.) can be measured and these kinetic energies also can be converted into the binding energies (B.E.) using the following equation [11].

$$K.E. = h\nu - B.E. - W \quad (2)$$

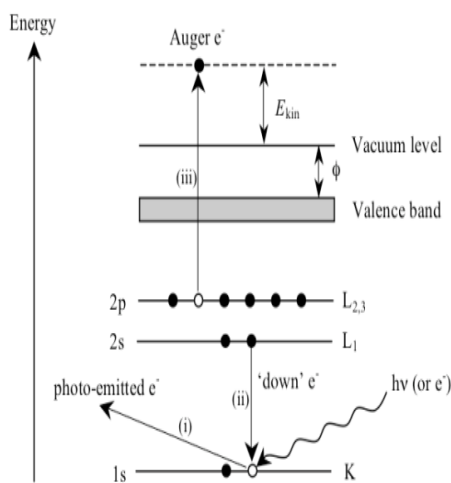


Fig (1): Photoemission process.

Ultra-High Vacuum (UHV)

The surface science experiments need to be conducted under a pressure of 10^{-9} mbar or lower. The ultrahigh vacuum (UHV) is required in order to prepare the surfaces without impurities [12] and reduces the number of molecules to interfere with the surface during the time frame of the experiment [7]. Therefore, to perform this type of experiment that should involve a chamber with series of pumps. To better understand the physical and chemical characteristics of material surfaces several techniques can be utilized such as X-ray photoelectron spectroscopy (XPS). The surface can be contaminated within 1 second at a pressure of 10^{-6} Torr [15] which is too short for the type of surface experiments whereas with the development of UHV at range pressure 10^{-10} mbar prevent surface contamination (e. g contamination by N_2 takes 79 hrs. to form at a pressure of 10^{-10} mbar) [7]. Therefore, the typical pressure of (UHV) is important to calculate. However, in similar conditions but at 10^{-10} mbar the mean free path is roughly estimated 106 m which is larger than the typical dimension of the chamber where those particles have more opportunities to be recorded for analysis [13].

$$\lambda = 1 / \sqrt{2} \pi d^2 n \quad (3)$$

Where d is the molecular diameter in meters, and n is the gas density in molecules per cubic meter. Mean free path for air at room temperature [14] is commonly used the following equation:

$$\lambda (cm) = 0.67 P(pa) \quad (4)$$

$$\lambda (cm) = 0.005 P(Torr) \quad (5)$$

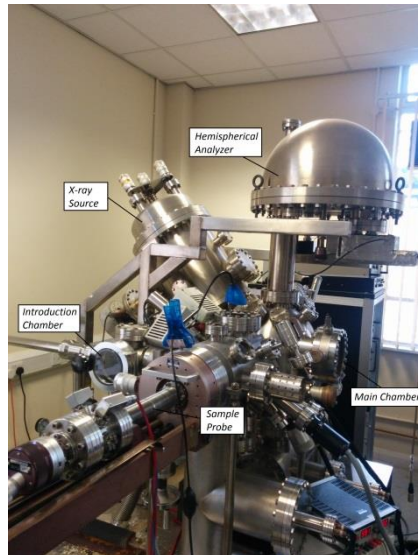


Fig (2): Schematics of UHV system.

Sputtering the surface to be roughed by using energetic (Ar^+) bombardment in order to remove any impurities remained on the surface in the form of oxides, organic carbide.... etc. [15] and the surface will be deformed chemically and structurally. Therefore, annealing cycles must be followed sputtering because required to regain the surface chemical composition and smoothness. Additionally, for annealing process the temperature and annealing time must be at an appropriate condition because any materials (sample) have a specific melting point. Therefore, keep in mind, once performing annealing samples [16]. Further to this, there is mass spectrometer also combined with chamber for screening if any unwanted gases still in the

chamber and the last system used to prepare chamber is an electron beam evaporator. Another part of UHV system is that the analysis chamber [14]. Whereas samples have been mounted in the chamber, those samples need to be transferred and checked during the experiment.

Results and discussion

Al-Cu-Fe QC

The results of the experiment in order to identify the chemical characteristics of quasi-crystal Al-Cu-Fe are described in tables (1) and (2) which display the various steps involved in this work. The XPS data were analysed by Casa XPS software, For this report Casa XPS will be carried out for elemental peak position identifying and to quantify the composition of surface (the percentage of concentration) of the sample typically, which for analysing the core level binding energy is used peak curve fitting based upon a Gaussian-Lorentzian curve which known as GL(X) and added to that Shirley background subtraction]. Furthermore, result of this study explained within these conditions and GL (30) was the natural line width on the instrument of XPS which is 0.3 eV of monochromatic source [17]. In spite of all these advantages point of the powerful analytical techniques which can be provided by using Casa XPS the opposite side has a few challenging cases, particularly for me as a beginner to use as briefly can be explained in terms of, in case of overlap peaks Al_{2p} and Cu_{3p} (Cu_{3p3/2}) which difficult to determine the contribution of Cu_{3p} in the concentration because this may affected to the composition of Al_{2p} in the surface of samples instead of Al_{2p} the chosen Al_{2s} is required that can be seen in Fig(3). Another tricky reason is that to identify peak position (2p, 2s and oxidation) in spectra could be inaccurate unless referenced to later literature of the same components of metal. The calculation of the chemical concentration of atom depends on the number of factors such as mean free path of an electron in metal λ_i , S_i is a sensitive factor of element i which known as Scofield Relative Sensitive Factor (ASF) or ionization cross-section of peak i [15, 18], defined as :

$$I_i = \lambda_i \sigma_i \quad (6)$$

$$C_i = 100\% \frac{(I_i/S_i)}{\sum_i I_i/S_i} \quad (7)$$

Where mean free path (IMFP) of a photoelectron can be varied based upon the kinetic energy of the photoelectron. As for calculating the concentration of Cu element in the surface could be as follows:

$$\% n_{Cu} = 100\% \frac{(I_{Cu}/S_{Cu})}{(I_{Al}S_{Al} + I_{Cu}S_{Cu} + I_{Fe}S_{Fe})} \quad (8)$$

Results of XPS scan

The Al _{2p} core level binding energy negatively charged to value that was compared to clean quasi-crystal at 72.9 eV [1], and in dirty sample which its value was 74.3 eV. In case which it is likely that indicator to the presence of Al oxide in dirty as a result of exposing to air. While the binding energy for the element Al 2p is 72.8 eV and 72.9 eV at clean quasi-crystal [19].

Table (1): Cleaning process of the experiment for Al-Cu-Fe QC.

Al-Cu-Fe	
Step	procedure
1	Dirty
2	1 st sputter
3	2 nd sputter
4	3 rd sputter
5	4 th sputter

Table (2): Results of XPS scan for Al-Cu- Fe QC.

element	Al2p	Fe2p	Cu2p	Al ₂ O ₃	Cu O	Cu LMM
	72.8 ⁽¹⁾	706.5 ⁽¹⁸⁾	932.5 ⁽¹⁸⁾	531.1 ⁽²⁷⁾	529-530 ⁽²⁷⁾	918.6 ⁽¹⁾
Step						
1	74.3	705.0	931.4	530.1	n/a	919.4
2	71.7	705.7	932.6	n/a	n/a	919.6
3	73.5	705.9	932.0	532.0	n/a	919.1
4	73.7	705.6	931.0	532.3	n/a	91.3
5	72.6	705.4	931.0	531.3	530.7	919.7

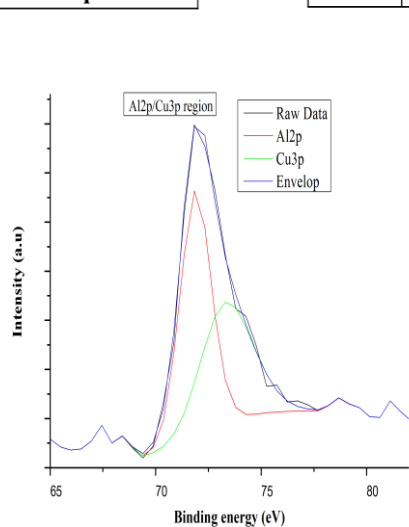


Fig (3):

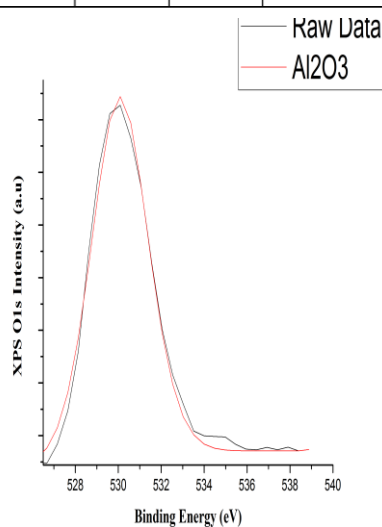


fig (4):

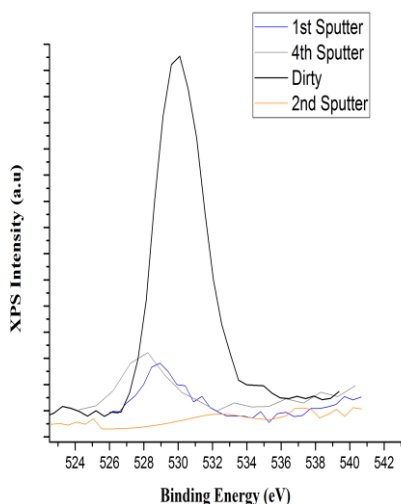


Fig (5): Cu2p region compered in 3 steps with dirty.

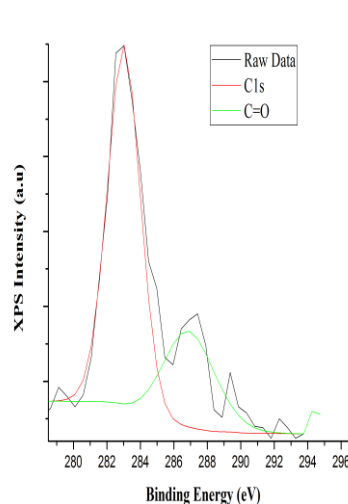


Fig (6): The contamination as on the sample.

Therefore, It is noticed that the existence of difficulties related to identify the oxide contributions when analysis this peak because due to its overlap with Cu_{2p}. Figure(2) The signal

of O1s at peak position 531.0 eV [19] that has been observed after 2st sputter which attributed to the presence of either Cu or Fe oxides at the surface, probably means that iron oxides because the charge has been transferred to 705.9 eV when comparing with 706.5 eV in clean quasi-crystal. Therefore, it confirms the absence of Al oxide which demonstrated by the composition percentage at Al 55%. This leads to confirm the presence Al metal in the subsurface region as sputtered, Fig (7a).

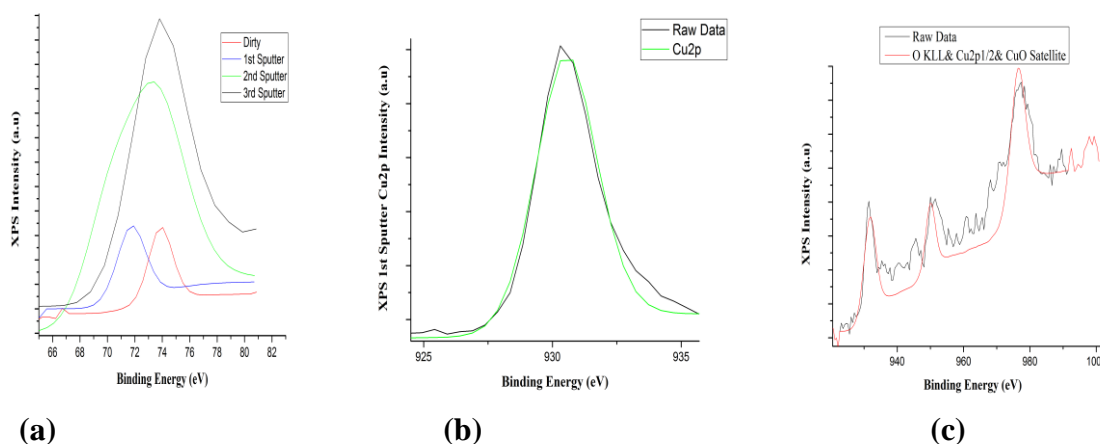


Fig (7): graphs display the effect of sputtering compared with cleaning process of Al2p, Cu2p 1st sputtered and cu2p in dirty sample.

The shift is noticed in the binding energies of Cu_{2p} was decreased (negatively charged) after 1st sputter which becomes 932.1eV and this was compared with copper metal at 932.5 eV [1] in clean quasi-crystal, Figure (7b) and in comparison region figure (7c). The Cu 2_p spectra is shifted to be similar as the binding energy of native Cu or Cu₂O roughly estimated 932.5 eV that references to the high resolution Cu 2_{p3/2} and to form oxidation, as given in literature [20] table (2). The evidence with respect to this phenomenon is exhibited in the composition in table (3) and Figure (8). However, the Cu LMM Auger transition can be affirmed this case. As the difference between the Cu LMM peaks for both element and oxide Cu₂O around 2 eV [7]. The Auger Cu LMM peak with respect to 2nd sputter has been obtained at the Kinetic energy 919.1 eV, as illustrated in fig (7c), which is not either belongs to (metal oxides) Cu LMM peak CuO or Cu₂O and those should be at 917.8 eV and 916.5 eV [7], respectively. The probability of which Auger Cu LMM peak refers to, re-confirms the existence of Cu metal at the subsurface.

The binding energy of iron Fe 2_p has been measured by the lower shift which were 706.6 eV at the dirty (exposed to air) and then positively shifted to 705.9 eV, 706.0 eV during the different times of sputtering. After sputtered under the pressure (3×10^{-9} mbar) for this experiment. Carbon has been reduced until its removed that evidenced from table (2) which was 235.0 eV at dirty and the surface was contaminated by C-O or C=O (carbon monoxide or carbon dioxide which need to use curve peak fitting to distinguish between their existence at the dirty surface). Fig (6), but eventually this contamination has been removed totally after sputtered, Figure (9). As long as the binding energy of Fe_{2p} is became 705.9 eV after 2nd sputter that represents the similar value of metal Fe as affirmed from Figure (9), suggests that the subsurface contains Fe metal as well.

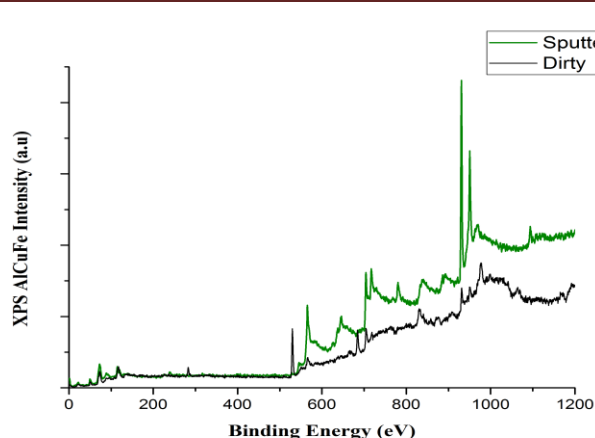


Fig (8): Survey Scan.

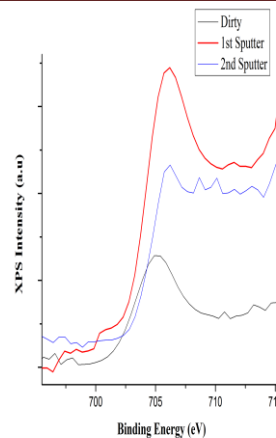


Fig (9): Fe 2p region.

The Al_{2p}, Cu_{2p} and Fe_{2p} (2p_{3/2}=2p) core level were used for calculating the composition and with respect to the percentage of surface concentration used by the relative sensitive factors [12] that found in the literature for Al, Pd and Mn as well. Therefore, the calculation of chemical composition was presented in table (3) which made be using Al_{2p} region. The uncertainty with respect to the measurement around 1-10%. Figure (10) the composition values have been represented in this plot show the values of the chemical composition when Al-Cu-Fe QC sputtered.

Table (3): The composition values of Al-Cu-Fe QC.

Composition%			
	Al	Cu	Fe
Step			
1	77	11	12
2	55	18	27
3	87	12	1
4	77	17	6
5	86	11	4

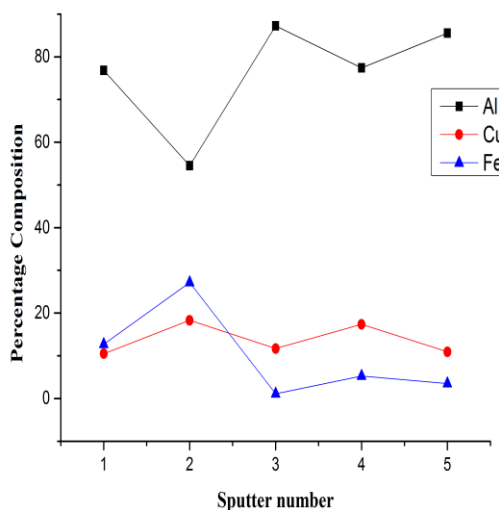


Fig (10): chemical composition when Al-Cu- Fe QC sputtered.

Al-Pd- Mn Quasicrystal sample

As previous mentioned the core level binding energy of either 2p or 3d refers to the 3/2 component, the outline of steps which have been conducted in this experiment by XPS technique as shown table (4) and the measurement results from it see table (Elemental composition analysis of sample Al-Pd-Mn QC).

Table (4): Scanning protocols of this experiment **Table (5): the region 2p of Al- pd- Mn sample.**

Al-Pd-Mn		element	Al2p	Pd3d	Pd 3d _{3/2}	Pd3p	Mn2p	Pd MNN
Step	procedure		72.8 ⁽¹⁾	335.5 ⁽³³⁾	340.3 ⁽²⁷⁾	532.4 ⁽³³⁾	638.8 ⁽³³⁾	327.4 ⁽³³⁾
1	Dirty							
2	1 st sputter	Step						
3	2 nd sputter	1	73.3	335.4	340.4	532.0	641.6	n/a
4	3 rd sputter	2	72.6	335.3	340.7	532.7	638.5	327.3
5	4 th sputter	3	71.7	335.9	340.8	532.3	638.0	327.7
6	5 th sputter	4	72.7	335.7	340.1	532.1	638.8	327.4
7	Sputtered- annealed	5	71.7	335.5	340.8	532.6	638.0	327.2
		6	71.8	335.5	340.7	532.3	638.3	327.7
		7	72.47	335.4	340.4	533.1	638.6	327.0

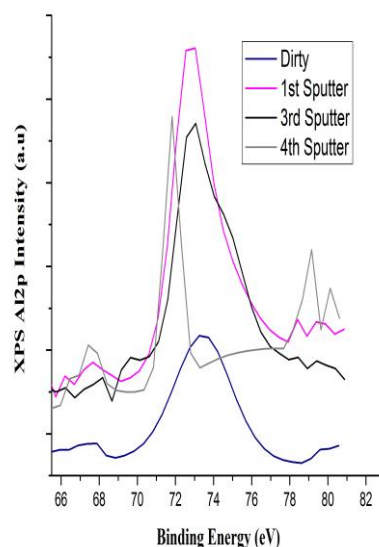


Fig (11): the shifts of peak position of Al_{2p} in Al-Pd-Mn QC.

It is clear that the peaks position at 73.0 eV belongs dirty sample Al-Pd-Mn QC Figure (11) and the observed shift has been shown in XPS spectra of Al_{2p}(due to the Al oxide which result from exposing to air).This figure displays the region comparison with other experiment in terms of peak position of Al_{2p}. There is a higher concentration of Al_{2p} which assumes its oxides layers to be on the surface 82% Al, arising regions of aluminium have been graphically appeared in Figure (4). By comprising with several sputtered and followed sputtered annealed process definitely evaluated from dirty sample. As noted that the dispersion of aluminium layers have been influenced by the cleaning processes which these binding energy decreased and the depletion of aluminium layer occurred, for example 72.6eV, 72.4eV and 72.7eV,

respectively. From the concentration percentages of Al- Pd- Mn QC as seen in Figure (10) shows insight into this depletion of Al % (69%, 6%, 25%). This may suggest that this confirms the presence of Al metal on the subsurface particularly step 4 and its oxides sputtered away, due to its preferential to be sputtered away and this means the absence of an oxide which resulted in the remaining of other content on the surface in case Pd.

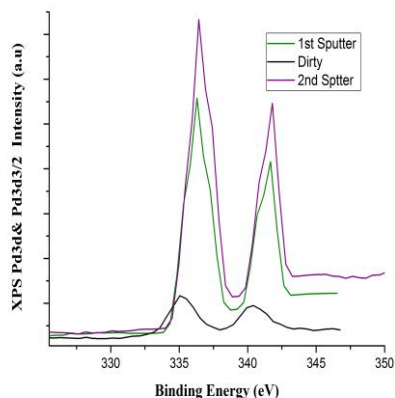


Fig (12): Pd_{3d} region evolution.

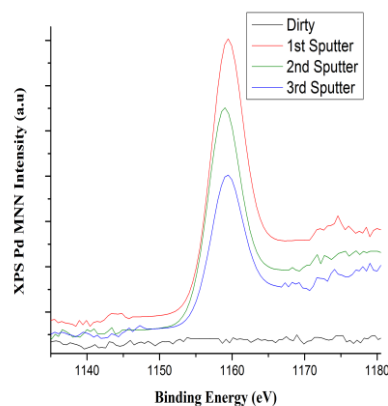


Fig (13): Auger peaks Pd MNN.

After 3rd sputter and sputtered –annealed Pd_{3d} were significantly positive charge 335.9eV and 335.4 eV, respectively in Fig. (12) . Corresponding to Auger peaks Pd MNN that were observed for both steps at 327.7eV and 327.0eV as shown Fig (13), respectively. Therefore, dramatic increases of the kinetic energies have been shown by comparing to the element 327.4eV [21] as Fig. (12) and ascribed to the detection both Pd and pd O. This predicted to the presence palladium and its oxide at the surface. However, the binding energies of Pd (3p_{1/2}& 3p_{3/2}) have been changed through the experiment procedures as described in table (5). O KLL Auger peak was seen clearly in the 1st sputter which could be attributed to the formation of Pd oxides (Pd O or Pd₂O) as its interfaced with O_{1s} at 531.0eV [7] but a look at binding energy Pd_{3p} 532.4eV. In spite of it was absence on the dirty and Pd O peak position at 532.7eV [14]. This suggests that the oxide may demonstrate its formation with Pd as well on the subsurface.

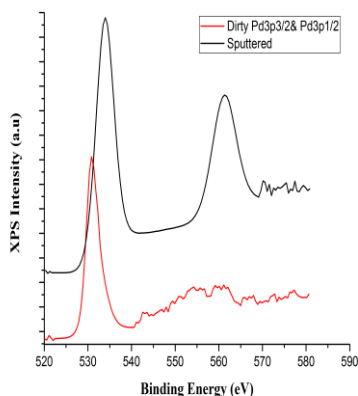


Fig (14):

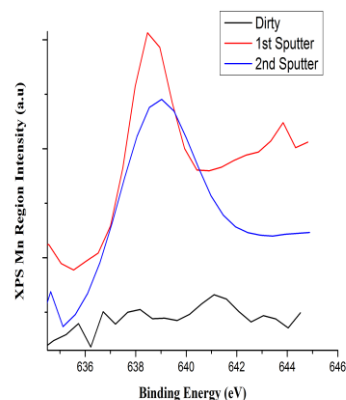


Fig (15): Mn_{2p} region.

The binding energies of Mn_{2p} were so complicated to identify as data drawn graphically Figure (15). Therefore, as seems of the dirty sample that oxides from air 641.1eV (643.0 ± 1.0 eV) [22] exhibits the oxidation form compared to element peak (639.0 ± 0.5 eV) [22] and resulting in the lowest concentration which in agreement with literature, and its composition in Al-Pd-Mn QC Mn% (0.1%). There was a chemical shift that has been appeared, which means positively charge the rough value of the binding energy 638.0eV after 2nd sputter corresponding to the composition 3% that can be noticed as Fig (16) and with respect to the concentration of Mn at the surface as taken from clean in UHV by sputtering and annealed was 5% that could be close to its concentration in the bulk 8% which in agree with scientific literature, from table (6) and overall composition ratio of step 6 was at 54: 34: 12 and could be represented the cleanest surface when compared to the compositional ratio of the bulk at 72: 20: 8, 70: 21: 21 [23] and [24], respectively. The uncertainty since each value was calculated in the composition around 0.1- 0.2eV. Furthermore, the surface became cleaned which can ease to observe from Fig. (17) and demonstrates the significant change that have been occurred on the dirty sample and after sputtering treatments.

Table (6): The composition calculated

Composition%			
	Al	Pd	Mn
Step			
1	86	12	2
2	74	20	6
3	43	54	3
4	74	21	5
5	87	10	3
6	54	34	12
7	69	6	25

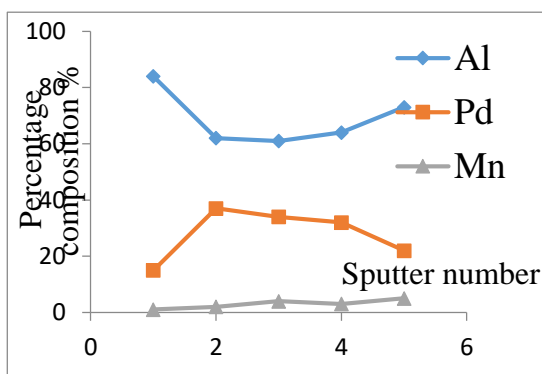


Fig (16): Elemental composition analysis of Sample Al-Pd-Mn QC

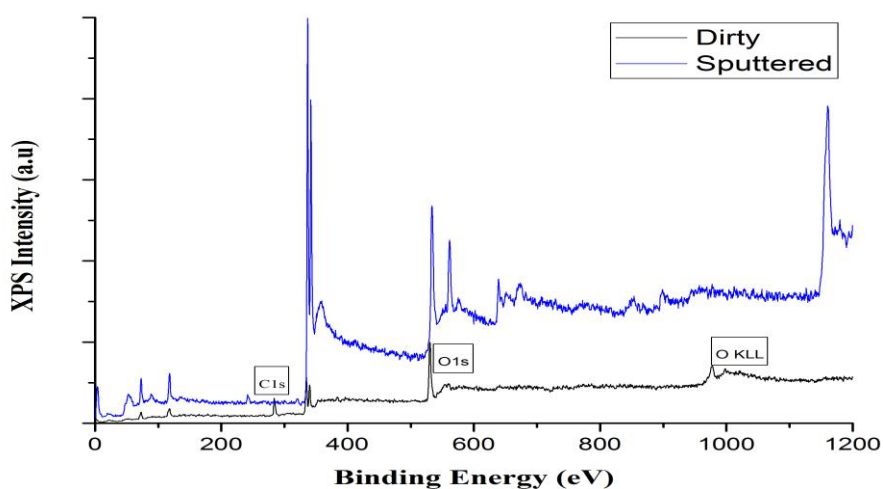


Fig (17): Survey scan of A-Pd-Mn QC

Al-Pd-Mn QC (Sputtered-annealed and deposit methanol)

The binding energies have been changed slightly in each component of Al-Pd-Mn QC when methanol (CH₃OH) decomposes at the surface of the quasi-crystal and analysis the data by casa XPS. The binding energy of core level Al2p once the sample sputtered and deposit 100L CH₃OH was obtained at 71.9 eV which lower than the binding energy of pure metal by 0.9eV, but after sputtered-annealed with deposit 100L and 1L CH₃OH observed a change between 72.7eV to 72.9eV. As indicated from the composition of Al was 72.88% which represents the highest percentage calculated when compared with Pd and Mn. The shifts of C_{1s} peaks that have been obtained under XPS in this experiment were found around 286.3eV, 286.9eV and 286.8eV, respectively.

Table (7):

element	Al2p	Pd3d	Mn2p	O1s	C1s
Process	72.8 ⁽¹⁾	335.5 ⁽³³⁾	638.8 ⁽³³⁾	531.0 ⁽¹⁾	284.9 ⁽¹⁾
Sputter+ 100L CH ₃ OH	71.9	335.9	638.1	532.7	286.3
Sputtered+ annealed+ 100L CH ₃ OH	72.7	337.3	638.7	532.2	286.9
Sputtered+ annealed+ 1L CH ₃ OH	72.9	337.2	638.8	532.8	286.8

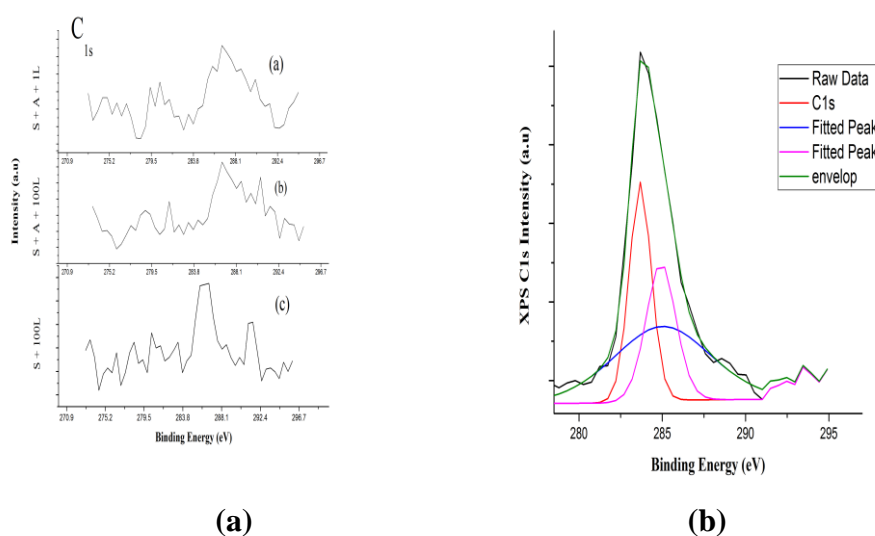


Fig (19):

However, these corresponding to C-O or C=O (as can be suggested that no clear which one is observed at the surface) which in agreement with literature. Methanol decomposes can be occurred at the surface which would appear to show that it produced from methanol Fig. (19): (a & b). As for Auger peaks illustrate a little difference as follow Figure (19 a). From photoelectron spectra of scan comparison of Al-Pd-Mn QC, once deposited methanol as seen in Fig.(20& 21), which the decomposition of methanol has been shown indicates the noteworthy feature that is taking place at the surface as evidenced early in discussion and supported by graphs.

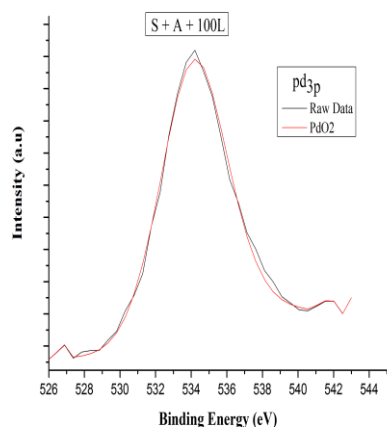


Fig ():

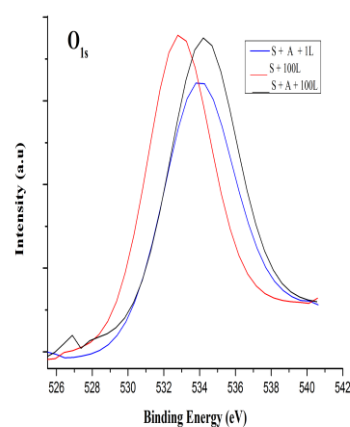


Fig ():

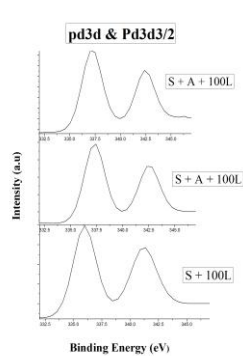
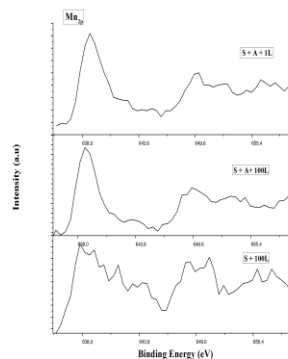


Fig ():



Conclusion

This study has attempted to identify the elements on the surface and the chemical composition of Al-Cu-Fe and Al-Pd-Mn quasi-crystals. Alteration to the composition of sputtering and sputtering -annealing treatment in order to determine the structure. Therefore, Al oxide on quasi-crystals has been removed during cleaning process which meant the absence of an oxide. The deposition of methanol at the Al-Pd-Mn quasi-crystal and leaching treatment with Na OH can be used to further explore the usage of these materials in the attractive application as catalyst for steam reforming of methanol. Measurements of peaks position of XPS spectra showed the presence of Pd oxide at the surface. Besides that, C1s shifts indicate methanol decomposition has taken place since deposit methanol.

References:

1. M. Lowe et al. J. Chem. Phys., 2015.
2. T. Tanabe and S. Kameoka and A. P. Tsai, Applied Catalysis A: General, 2010, Microstructure of Leached Al-Cu-Fe Quasicrystal with High Catalytic Performance for Steam Reforming of Methanol,
3. S. Kameoka et al, Catalysis Today, 2004.
- 4.M. Yoshimura et al, Journal of Alloys and Compounds, 2002.
5. A. P. Tsai et al. Applied Catalysis A-General, 2001.
- 6.T. Tanabe et al. Journal of Materials Science, (2011).
7. E.B. Ferre, journal of physics Condensed Matter, 2002.
- 8.M. N. Gilmour, PhD Thesis, 2010.
9. C. J. Jenks et al, Article (A short Review from a surface Science Perspective, 1998.
10. Y. Matsumura et al, Catalysis letters, 1997.
11. D. Butcher, PhD thesis, 2010.
12. J. Russell et al, Book, LENNEX Corp, 2012.
13. .P. James et al, PhD thesis, 2000.
- 14.L. Wearing, PhD Thesis, the University of Liverpool, Formation of metallic over layers on quasicrystal surfaces, 2008.
15. D. Briggs, Book Surface ANAL of polymers by XPS, 1998.
14. H. Luth, Master thesis, 2010.
15. K. S. Kim et al, Analytical Chemistry, 1974.
16. D. R. Butcher, In Situ Studies of Surface Mobility on Nobel Metal Model catalysts Using STM, PhD Thesis, University of California and Berkeley, 2010.
17. J. W. Niemantsverdriet , Spectroscopy in Catalysis An introduction, WILEY-VCH Verlag GmbH & Co.KgaA,2007
18. Zorn et al, G. Zorn and S. R. Dave and X. Gao and D. G. Castner New Method for Determining the Elemental Composition and Distribution in Semiconductor Core-Shell Quantum Dots, research article, Anal Chem, 2011.
19. B. Zotriazole et al, Corrosion inhabitation of Cu-Ni(90/10) Alloy in sea water and sulphide-Polluted sea water Environments, Research Article, 2013.
20. J. F. O` Hanlon, A User`s Guide to Vacuum Technology, A JOHN WILEY \& SONS, INC, 2003.
- Coates,
22. R. Reiche et al, Applied surface science, 2001.
23. B. Brun et al, journal of electron spectroscopy and related phenomena, 1999.
24. C. Jenks et al, condensed matter and material physics1996.